

1 Increasingly powerful tornadoes in the United States

2 James B. Elsner¹, Tyler Fricker¹, Zoe Schroder¹

3 ¹Department of Geography, Florida State University, Tallahassee, FL 32306, USA

4 **Key Points:**

- 5 • Tornadoes in the United States appear to be getting more powerful.
- 6 • The upward trend is independent of occurrence time and changes to the damage
7 scale.
- 8 • Part of the trend is linked to increases in CIN and to CAPE conditional on
9 increasing shear.

Corresponding author: James B. Elsner, jelsner@fsu.edu

Abstract

Storm reports show an upward trend in the power of tornadoes from longer and wider paths and higher damage ratings. Quantifying the magnitude of the increase is difficult given diurnal and seasonal influences on tornadoes embedded within natural variations and made worse by changes in practices for rating damage. Here the authors solve this problem by fitting a statistical model to a metric of tornado power during the period 1994–2016. They find an increase of 5.5% [(4.6, 6.5%), 95% CI] per year in power controlling for the diurnal cycle, seasonality, natural climate variability, and the switch to a new damage scale. A portion of the trend is attributed to long-term changes in convective storm environments involving dynamic and thermodynamic variables and their interactions. Increasing power is occurring in environments where the effect of convective available potential energy is enhanced by increasing vertical wind shear.

1 Introduction

Tornadoes are nature’s most violent storms with winds that can exceed 120 m s^{-1} . A mobile Doppler radar estimated a near-ground-level wind speed of 135 m s^{-1} in the Bridge Creek-Moore, Oklahoma tornado of May 3, 1999. How global warming will affect tornadoes remains an open question. It has been argued that because of data inadequacy and limited physical understanding of the processes that cause tornadoes it is difficult to detect trends related to climate change (Kunkel et al., 2013). However this argument is based on studies that are at least five years old, focus exclusively on tornado occurrences, and use methods that lack ways to include intervening factors at multiple levels (e.g., hourly and seasonal). Here we focus on tornado power and use a hierarchical statistical model that controls for the known behavior of tornado activity.

We begin by noting that while the annual number of strong and violent tornadoes (EF2 or worse) has remained relatively consistent from year to year, the number of days with many tornadoes is on the rise (Brooks, Carbin, & Marsh, 2014; Elsner, Elsner, & Jagger, 2015; Tippett, Lepore, & Cohen, 2016; Tippett, Sobel, Camargo, & Allen, 2014). An increase in the number of big tornado days implies a larger threat of damaging tornadoes (Elsner, Jagger, Widen, & Chavas, 2014) with the percentage of violent tornadoes (EF4 or worse) increasing with increasing outbreak size (number of tornadoes). On days with 16 to 31 tornadoes less than 4% of the tornadoes are rated EF3 or worse while on days with more than 63 tornadoes more than 8% of the tornadoes are rated EF3 or worse (Table 1). Increased percentages of violent (EF4 and EF5) tornadoes with increasing tornado-day size occur as well. This leads us to hypothesize that tornadoes are becoming more powerful.

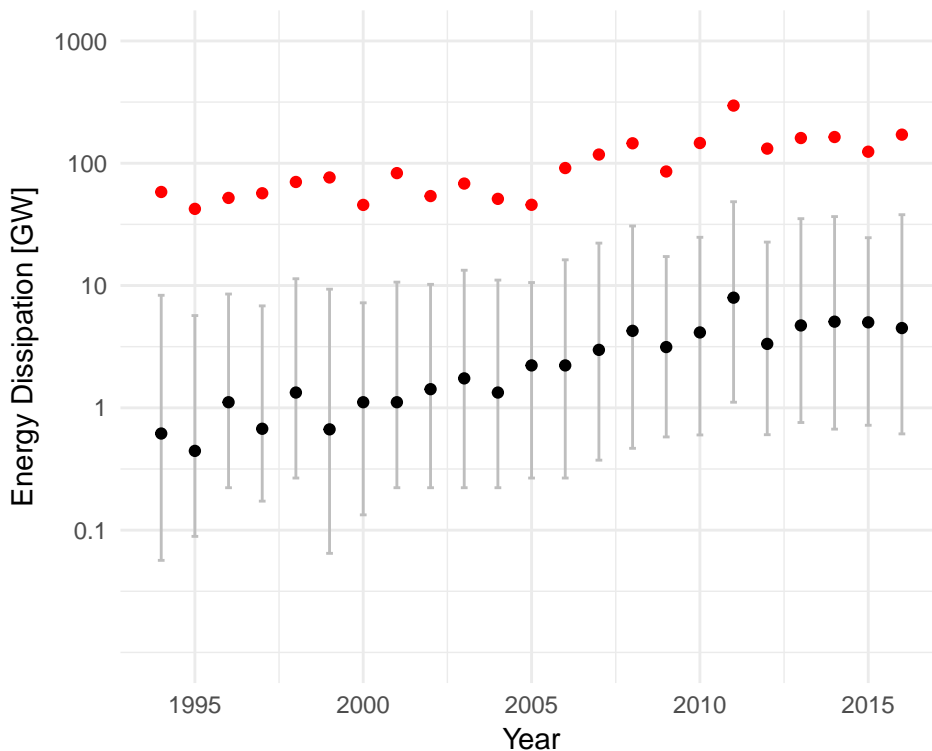
Table 1. Tornado statistics by tornado-day size. Numbers are based on all tornado reports over the period 1994–2016. Data are from the Storm Prediction Center.

Tornado Day Size (No. Tor.)	Number of Cases	Total Number of Tor.	% Tor. Rated Intense (EF3+)	% Tor. Rated Violent (EF4+)
1	1088	1088	0.37	0.00
2-3	1068	2581	0.39	0.00
4-7	874	4521	0.82	0.09
8-15	644	6921	1.99	0.38
16-31	295	6466	3.34	0.57
32-63	103	4355	5.49	1.08
>63	25	2018	8.18	2.23

2 Results

Tornado power is metered by the energy dissipated near the ground (Fricker, Elsner, & Jagger, 2017). On average, the longest lasting tornadoes generate the most extreme wind speeds (Brooks, 2004; Elsner, Jagger, & Elsner, 2014; Fricker & Elsner, 2015). And indeed, damage paths are getting longer (see Appendix Fig. A1). Multiplying path area, air density, and wind speed gives an estimate of the total energy dissipated by a tornado (Fricker et al., 2017) (See §Methods). For the set of 27,950 tornadoes during the period 1994–2016, the median power is 2.22 gigawatts (GW) with an inter-quartile range between .27 and 17 GW. Tornado power is highly correlated ($r > .9$) with the destructive potential index developed at the U.S. Storm Prediction Center (SPC) (Fricker & Elsner, 2015) and with the number of casualties when people are present (Fricker et al., 2017). The Tallulah-Yazoo City-Durant tornado (Louisiana and Mississippi) of 24 April 2010 that killed ten and injured 146 had an estimated power of 66,200 GW. Annual statistics of tornado power show clear upward trends with the median, quartiles, and 90th percentile all on the rise over the period 1994–2016 (Fig. 1).

Figure 1. Annual energy dissipation (power) by year. The black dot is the median and the red dot is the 90th percentile value each year. The vertical bar extends from the lower to upper quartile numbers.

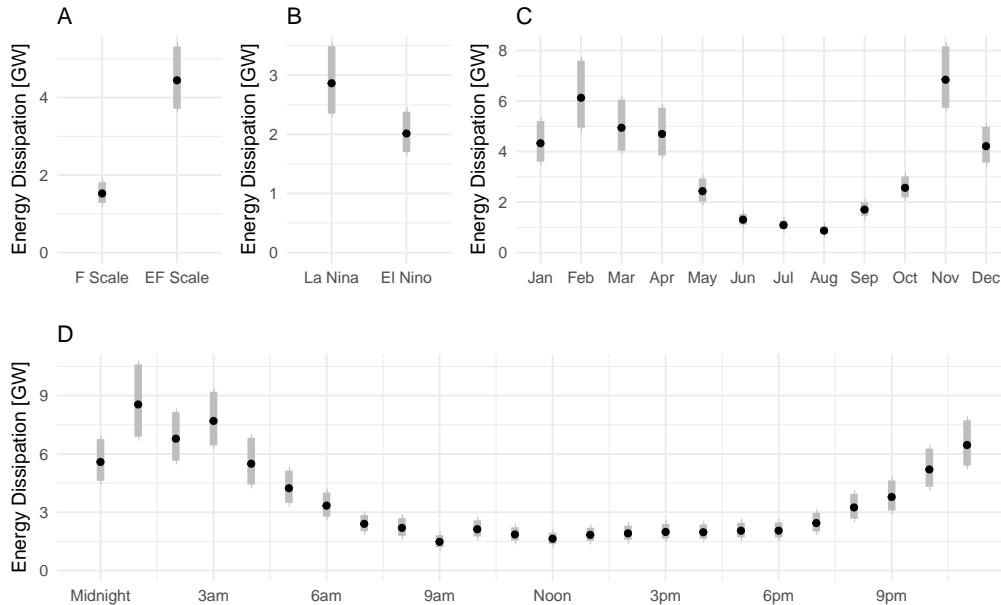


The observed increase in power might be the result of shifts in when and where tornadoes occur (Agee, Larson, Childs, & Marmo, 2016). Also, at least a portion of the rise is due to a change in the procedures to rate the damage left behind. The EF damage rating scale was revised from the original F scale (and was put into operational use in 2007) with better standards for determining what was previously subjective including additional structures and vegetation, expanded degrees of damage, and a better accounting of construction quality. Figure 2 shows tornado power grouped by

68 the change in the EF rating scale (A), El Niño/La Niña (B), month of occurrence (C),
 69 and by time of day (D). Mean energy dissipation (power) is relatively higher at night,
 70 during La Niña, in the cooler months, and after the implementation of the EF rating
 71 procedure.

72 To test our hypothesis of an upward trend in tornado power, after accounting
 73 for these known influences, we fit a hierarchical regression model to the per-tornado
 74 power using all available tornado reports over the period 1994–2016. The model has
 75 a log-normal distribution for the likelihood on the per-tornado power where a lower
 76 bound is set at .444 GW; a value just below the least powerful tornado in the record.
 77 Fixed effects in the model include the bivariate index for ENSO and a variable to
 78 mark the year when the switch to the new damage rating procedures were put in place
 79 (2007). Random effects include month and hour to capture the cyclic change in energy
 80 at these respective time scales. A term indexing the year of occurrence is included as
 81 a fixed effect to test our hypothesis and to quantify the residual trend per annum (see
 82 §Methods).

Figure 2. Energy dissipation (power) grouped by EF change, ENSO, month, and hour. The dot is the geometric mean for each subgroup and the gray bars extend one standard deviation from the mean.



83 As expected the model shows the cycle of alternating ocean-atmosphere conditions
 84 in the equatorial Pacific, known as ENSO, is an important and significant
 85 influence on tornado power with a regression coefficient expressed as a multiplicative
 86 decrease of .93 [(.90, .96), 95% CI] (exponentiating the coefficient in Table 2) for every
 87 one standard deviation increase (going from La Niña to El Niño) in the bivariate
 88 ENSO index. This is consistent with the fact that under La Niña conditions (especially
 89 during winter) amplified upper-air troughs move across North America. This results
 90 in warmer than normal temperatures in the Southeast and cooler than normal temperatures
 91 in the Northwest, which sets the stage for severe weather outbreaks that are
 92 intensified by a strong jetstream (Allen, Tippett, & Sobel, 2015; Cook, Leslie, Parsons,
 93 & Schaefer, 2017; Cook & Schaefer, 2008). The model also shows that the procedures
 94 put in place following the adoption of the EF damage rating scale results in an increase

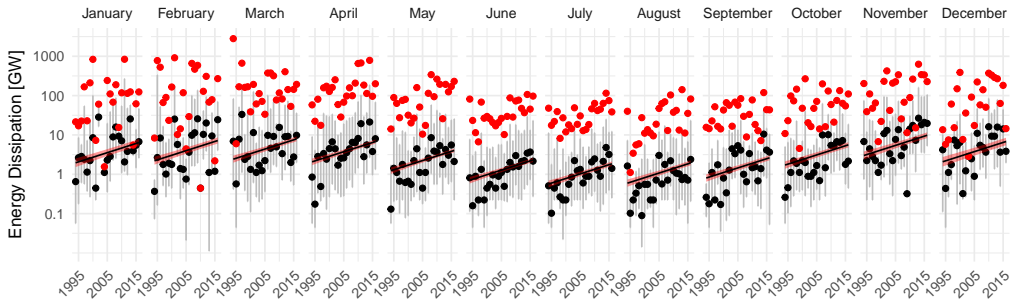
95 in power by a factor of 1.41 [(1.24, 1.59), 95% CI]. This increase is expected given the
 96 improvements after adoption in damage surveys including more precise and inclusive
 97 damage indicators.

Table 2. Fixed effects. Estimated coefficients on the fixed effects terms in the model. The Error is one standard deviation. The lower and upper 95% credible intervals are given.

	Estimate	Error	l-95% CI	u-95% CI
α	21.298	0.023	21.253	21.344
β_{ENSO}	-0.068	0.016	-0.101	-0.036
$\beta_{\text{EF?}}$	0.341	0.063	0.217	0.462
β_{Year}	0.054	0.005	0.045	0.063

98 Most importantly the model shows a significant upward trend in tornado power
 99 at a rate of 5.5% [(4.6, 6.5%), 95% CI] per year. The magnitude of the increase depends
 100 on the data and the model that controls for diurnal and seasonal variability, the ENSO
 101 cycle, and implementation of the EF rating scale. The model quantifies the increasing
 102 ferocity of tornadoes independent of the other factors considered and lends support
 103 to our hypothesis that as tornado days become larger the tornadoes themselves are
 104 becoming more powerful. The base rate from which the upward trend depends on the
 105 time of the year through the random-effect term, but the monthly trends appear to
 106 track the data well (Fig. 3).

Figure 3. Upward trends in energy dissipation (power) by month. The black dot is the median and the red dot is the 90th percentile value each year. The vertical bar extends from the lower to upper quartile numbers. The black line is the modeled trend with a 95% CI band shown in red shading.



107 3 Discussion

108 The study is retrospective but our hierarchical modeling strategy can help un-
 109 cover clues about what might be happening as the earth warms. We conjecture
 110 that at least a portion of the upward trend in tornado power is related to long-term
 111 changes in regional environments associated with severe thunderstorms. Modeling
 112 studies project increases in convective available energy (CAPE) with a warmer cli-
 113 mate (DelGenio, Yao, & Jonas, 2007; Diffenbaugh, Scherer, & Trapp, 2013; Trapp,
 114 Diffenbaugh, & Gluhovsky, 2009), and we previously hypothesized that climate change
 115 and increases in CAPE could be leading to more active areas of severe convection on

116 days with tornadoes (Elsner, Jagger, & Elsner, 2014). Increases in CAPE with global
 117 warming are documented in both climate models (Sobel & Camargo, 2011) and cloud-
 118 system-resolving models (Romps, 2011), and these increases have theoretical support
 119 (Seeley & Romps, 2015; Singh & O’Gorman, 2013).

120 Here we examine how regional environmental factors including CAPE, convective
 121 inhibition (CIN), and storm relative helicity (SRH) are related to the trend in tornado
 122 power. We use gridded reanalysis data at 1800 UTC on big tornado days with at least
 123 ten tornadoes (there are 748 big days in the period January 1994 through September
 124 2014). We spatially average each of the three environmental variables separately over
 125 all grid point values within the domain defined by all the tornado genesis locations
 126 for that day. Averages over all outbreak days by year show upward trends in SRH
 127 (Tippett et al., 2016) and CIN (Fig. 4[B & C]). We include the environmental variables
 128 in models for average tornado power (averaged over all tornadoes in the outbreak and
 129 divided by the area of the domain) and find the best model when CAPE and SRH are
 130 used as an interaction term. In other words, the model indicates that CAPE’s effect on
 131 tornado power is significantly enhanced with increasing SRH (Fig. 4[A]). For example,
 132 with average SRH values at 100 J/kg tornado power increases by 18% per 1000 J/kg
 133 of CAPE but with average SRH values of 250 J/kg power increases by 55% for the
 134 same 1000 J/kg of CAPE. The conditionality in the effect of CAPE on SRH is not
 135 detectable if we analyze the data without the interaction term, since in this case the
 136 model assumes that the relationship of tornado power with respect to CAPE and SRH
 137 is the same regardless of the value of the other variable. Importantly the magnitude
 138 of the trend in a model that includes the three environmental variables is 24% lower
 139 compared with the magnitude of the trend in a model that excludes them. Thus we
 140 conclude that increasing tornado power is occurring in environments with increasing
 141 CIN and in environments where the effect of CAPE is being enhanced by increasing
 142 SRH.

143 In summary, we identified an upward trend in tornado power (computed from
 144 the official records) after accounting for known factors and then demonstrated that
 145 a portion of the trend is statistically related to CAPE conditional on SRH. More
 146 definitive answers to important questions concerning climate change and tornadoes
 147 will need to wait for a better theoretical understanding of tornado processes. But, the
 148 large number of tornadoes that occur each year provides a generous sample that allows
 149 researchers to use hierarchical models to separate potential climate-change signals from
 150 noise.

151 4 Methods

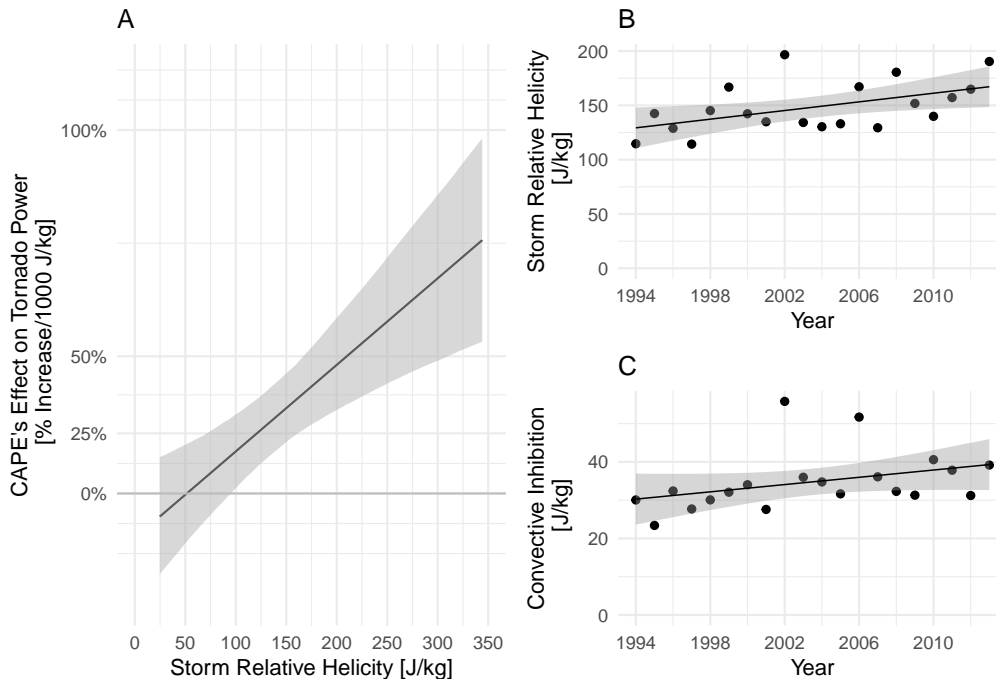
152 4.1 Tornado power (energy dissipation)

We calculate tornado power (P) using the energy dissipation equation defined in Fricker et al. (2017) as:

$$P = A_p \rho \sum_{j=0}^5 w_j v_j^3, \quad (1)$$

153 where the summation is over the six possible EF ratings (0, 1, 2, 3, 4 and 5), A_p is
 154 the area of the tornado’s path [units of square meters], ρ is air density [1 kg m^{-3}],
 155 v_j is the midpoint wind speed [m s^{-1}] for each damage rating (EF scale) j , w_j is
 156 the corresponding fraction of path area by damage rating. Multiplying the units
 157 from the individual terms results in P having units of power [$\text{kg m}^2 \text{ s}^{-3} = \text{Joule/s} =$
 158 Watt (W)]. Path area is the product of path width and path length. Path length is
 159 known to a relatively high degree of accuracy (Doswell, Edwards, Thompson, Hart,
 160 & Crosbie, 2006). Path length and width and maximum EF rating are listed in the
 161 Storm Prediction Center’s tornado database.

Figure 4. Upward trends in storm relative helicity (SRH), convective inhibition (CIN), and the conditional effect of convective available potential energy (CAPE). The sloping black lines denote point estimates of the trends and the gray ribbons indicate the 95% uncertainty bound around the point estimates.



162 The database is compiled from the National Weather Service's (NWS) *Storm*
 163 *Data*, and includes all known tornadoes dating back to 1950. Here we focus on the
 164 available recent period of this record from 1994–2016. The start year of 1994 marks the
 165 beginning of the extensive use of the WSR-88D radar. The fraction of path area is that
 166 recommended by the U.S. Nuclear Regulatory Commission (Fricker & Elsner, 2015),
 167 which combines a Rankine vortex with empirical estimates derived from detailed storm
 168 surveys (Ramsdell & Rishel, 2007). Threshold wind speeds for the EF ratings are a
 169 three second gust. With no upper bound on the EF5 wind speeds, the midpoint wind
 170 speed is set at 97 m s^{-1} (7.5 m s^{-1} above the threshold wind speed consistent with the
 171 EF4 midpoint speed relative to its threshold). Tornado power is highly correlated with
 172 the destructive potential index (Fricker & Elsner, 2015; Thompson & Vescio, 1998).
 173 Additional details and justification for using tornado power are given in Fricker et al.
 174 (2017). Power by EF rating is given in Table 3.

175 4.2 ENSO and environmental variables

176 The ENSO variable is the bi-variate ENSO (BEST) monthly series that uses a
 177 combination of the standardized Southern Oscillation Index (SOI) with a standardized
 178 Niño 3.4 sea-surface temperature (SST) series. We download values of the series from
 179 the Earth System Research Laboratory, Physical Science Division (NOAA/OAR/ESRL
 180 PSD). Environmental variables including CAPE, CIN, and SHR are from National Cli-
 181 matic Data Centers (NCDC) North American Regional Reanalysis (NARR) dataset,
 182 which is also available from ESRL PSD. Each NARR file is available as a 277 by
 183 349 rectangular raster that encompasses the entire United States. We download the

Table 3. Tornado power by EF rating. Numbers are in gigawatts (GW) and are based on the 27,950 tornadoes over the period 1994–2016.

(E)F Rating	n	Median	Total	Arithmetic Mean	Geometric Mean
0	17182	0.5	73329.6	4.3	0.6
1	7735	12.5	364162.5	47.1	10.8
2	2224	91.4	609230.8	273.9	77.5
3	650	615.7	827474.3	1273.0	495.4
4	145	1631.0	511177.8	3525.4	1427.6
5	14	6458.5	130239.0	9302.8	5622.7

184 18UTC data for each big day because tornado activity generally peaks in the early
 185 afternoon. The available NARR dataset ends in September 2014 so we use only the
 186 big days that occur between January 1994 and September 2014.

187 4.3 Statistical models

188 For each tornado a log-normal distribution is assumed for power with a lower
 189 bound set to .444 GW. The geometric means of the distributions are logically related
 190 to the fixed effects and their coefficients (β 's) including year of occurrence, the bivariate
 191 ENSO index, and an indicator variable to mark the year when the switch to the new
 192 damage rating procedures were put in place (2007). Variations in power by month
 193 and hour are modeled as random intercept effects so the corresponding coefficients
 194 are vectors of length 12 and 24, respectively. Mathematically the regression model is
 195 expressed as:

$$\ln(P|P > 444000) = \alpha + \beta_{\text{Year}}\text{Year} + \beta_{\text{ENSO}}\text{ENSO} + \beta_{\text{EF?}}\text{EF?} + \beta_{\text{Month}}(1|\text{Month}) + \beta_{\text{Hour}}(1|\text{Hour})$$

196 To examine the influence environmental variables including CAPE, CIN, and
 197 SRH have on reducing the upward trend, a similar regression model is fit to power per
 198 unit area averaged over all tornadoes on a day with at least ten tornadoes. A model
 199 using outbreak-level data (rather than tornado-level data) is needed because the scale
 200 of individual tornadoes is much smaller than the scale at which the environmental
 201 variables are resolved. Here values for the environmental variables on a regular grid
 202 are averaged over a convex polygon domain enclosing all the tornado genesis locations
 203 for that day. The best model (lowest Akaike information criterion (AIC) value) includes
 204 CIN and an interaction between CAPE and SRH.

205 4.4 Code and data archive

206 Analysis and modeling are performed using the software environment R (<http://www.r-project.org>). Models are fit using maximum likelihood procedures with functions in the **lme4** package (Bates, Mächler, Bolker, & Walker, 2015) and using Bayesian simulations in the Stan computational framework (<http://mc-stan.org/>) accessed through the **brms** package (Bürkner, 2017). When using Bayesian simulations we specified mildly informative conservative priors to improve convergence and guard against over-fittings. The codes and data to reproduce the results from this study are available here <https://github.com/jelsner/tor-pwr-up> and here

214 <https://github.com/jelsner/get-NARR>. The NARR and ENSO data are provided
 215 by the NOAA/OAR/ESRL PSD, Boulder, Colorado, USA at [https://www.esrl.noaa](https://www.esrl.noaa.gov/psd/)
 216 [.gov/psd/](https://www.esrl.noaa.gov/psd/).

217 Acknowledgments

218 The code and data to reproduce the results from this study are available from [https://](https://github.com/jelsner/tor-pwr-up)
 219 github.com/jelsner/tor-pwr-up and <https://github.com/jelsner/get-NARR>.

220 References

- 221 Agee, E., Larson, J., Childs, S., & Marmo, A. (2016, 05). Spatial redistribution of
 222 USA tornado activity between 1954 and 2013. *Journal of Applied Meteorology*
 223 *and Climatology*, *55*, 1681-1697.
- 224 Allen, J. T., Tippett, M. K., & Sobel, A. H. (2015). Influence of the El
 225 Niño/Southern Oscillation on tornado and hail frequency in the United States.
 226 *Nature Geosciences*, *8*, 278-283.
- 227 Bates, D., Mächler, M., Bolker, B., & Walker, S. (2015). Fitting linear mixed-effects
 228 models using lme4. *Journal of Statistical Software*, *67*(1), 1-48. doi: 10.18637/
 229 jss.v067.i01
- 230 Brooks, H. E. (2004). On the relationship of tornado path length and width to in-
 231 tensity. *Weather and Forecasting*, *19*, 310-319.
- 232 Brooks, H. E., Carbin, G. W., & Marsh, P. T. (2014). Increased variability of
 233 tornado occurrence in the united states. *Science*, *346*(6207), 349-352. Re-
 234 trieved from <http://science.sciencemag.org/content/346/6207/349> doi:
 235 10.1126/science.1257460
- 236 Bürkner, P.-C. (2017). brms: An R package for bayesian multilevel models using
 237 Stan. *Journal of Statistical Software*, *80*(1), 1-28. doi: 10.18637/jss.v080.i01
- 238 Cook, A. R., Leslie, L. M., Parsons, D. B., & Schaefer, J. T. (2017, sep). The im-
 239 pact of el niño-southern oscillation (ENSO) on winter and early spring u.s.
 240 tornado outbreaks. *Journal of Applied Meteorology and Climatology*, *56*(9),
 241 2455-2478. Retrieved from <https://doi.org/10.1175/jamc-d-16-0249.1>
 242 doi: 10.1175/jamc-d-16-0249.1
- 243 Cook, A. R., & Schaefer, J. T. (2008). The relation of El Niño-Southern Oscilla-
 244 tion (ENSO) to winter tornado outbreaks. *Monthly Weather Review*, *136*,
 245 3121-3137.
- 246 DelGenio, A. D., Yao, M.-S., & Jonas, J. (2007, aug). Will moist convection be
 247 stronger in a warmer climate? *Geophysical Research Letters*, *34*(16). Retrieved
 248 from <https://doi.org/10.1029/2007gl030525> doi: 10.1029/2007gl030525
- 249 Diffenbaugh, N. S., Scherer, M., & Trapp, R. J. (2013). Robust increases in se-
 250 vere thunderstorm environments in response to greenhouse forcing. *Pro-*
 251 *ceedings of the National Academy of Sciences*, *110*, 16361-16366. doi:
 252 10.1073/pnas.1307758110
- 253 Doswell, C. A., Edwards, R., Thompson, R. L., Hart, J. A., & Crosbie, K. C. (2006,
 254 dec). A simple and flexible method for ranking severe weather events. *Weather*
 255 *and Forecasting*, *21*(6), 939-951. Retrieved from [https://doi.org/10.1175/](https://doi.org/10.1175/waf959.1)
 256 [waf959.1](https://doi.org/10.1175/waf959.1) doi: 10.1175/waf959.1
- 257 Elsner, J. B., Elsner, S. C., & Jagger, T. H. (2015). The increasing efficiency of tor-
 258 nado days in the United States. *Climate Dynamics*, *45*(3-4), 651-659.
- 259 Elsner, J. B., Jagger, T. H., & Elsner, I. J. (2014). Tornado intensity estimated from
 260 damage path dimensions. *PLoS ONE*, *9* (9), e107571.
- 261 Elsner, J. B., Jagger, T. H., Widen, H. M., & Chavas, D. R. (2014). Daily tornado
 262 frequency distributions in the United States. *Environmental Research Letters*,
 263 *9*(2), 024018.
- 264 Fricker, T., & Elsner, J. B. (2015). Kinetic energy of tornadoes in the United States.

- 265 *PLoS ONE*, 10, e0131090. doi: 10.1371/journal.pone.0131090
- 266 Fricker, T., Elsner, J. B., & Jagger, T. H. (2017). Population and energy elasticity of
267 tornado casualties. *Geophysical Research Letters*, 44, 3941-3949. doi: 10.1002/
268 2017GL073093
- 269 Kunkel, K. E., Karl, T. R., Brooks, H., Kossin, J., Lawrimore, J. H., Arndt, D.,
270 ... Wuebbles, D. (2013, apr). Monitoring and understanding trends in
271 extreme storms: State of knowledge. *Bulletin of the American Meteorolog-
272 ical Society*, 94(4), 499-514. Retrieved from [https://doi.org/10.1175/
273 bams-d-11-00262.1](https://doi.org/10.1175/bams-d-11-00262.1) doi: 10.1175/bams-d-11-00262.1
- 274 Ramsdell, J. V., Jr, & Rishel, J. P. (2007, February). *Tornado Climatology of the
275 Contiguous United States* (Tech. Rep. Nos. NUREG/CR-4461, PNNL-15112).
276 P.O. Box 999, Richland, WA 99352: Pacific Northwest National Laboratory.
- 277 Romps, D. M. (2011, jan). Response of tropical precipitation to global warm-
278 ing. *Journal of the Atmospheric Sciences*, 68(1), 123-138. Retrieved from
279 <https://doi.org/10.1175/2010jas3542.1> doi: 10.1175/2010jas3542.1
- 280 Seeley, J. T., & Romps, D. M. (2015, nov). Why does tropical convective avail-
281 able potential energy (cape) increase with warming? *Geophysical Research
282 Letters*, 42(23), 10,429-10,437. Retrieved from [https://doi.org/10.1002/
283 2015GL066199](https://doi.org/10.1002/2015GL066199) doi: 10.1002/2015GL066199
- 284 Singh, M. S., & O’Gorman, P. A. (2013, aug). Influence of entrainment on the ther-
285 mal stratification in simulations of radiative-convective equilibrium. *Geophys-
286 ical Research Letters*, 40(16), 4398-4403. Retrieved from [https://doi.org/10
287 .1002/grl.50796](https://doi.org/10.1002/grl.50796) doi: 10.1002/grl.50796
- 288 Sobel, A. H., & Camargo, S. J. (2011, jan). Projected future seasonal changes in
289 tropical summer climate. *Journal of Climate*, 24(2), 473-487. Retrieved from
290 <https://doi.org/10.1175/2010jcli3748.1> doi: 10.1175/2010jcli3748.1
- 291 Thompson, R., & Vescio, M. (1998). The Destruction Potential Index - A Method
292 for Comparing Tornado Days. In *19th conference on severe local storms*.
- 293 Tippett, M. K., Lepore, C., & Cohen, J. E. (2016, dec). More tornadoes in
294 the most extreme u.s. tornado outbreaks. *Science*, 354(6318), 1419-
295 1423. Retrieved from <https://doi.org/10.1126/science.aah7393> doi:
296 10.1126/science.aah7393
- 297 Tippett, M. K., Sobel, A. H., Camargo, S. J., & Allen, J. T. (2014). An empirical
298 relation between U.S. tornado activity and monthly environmental parameters.
299 *Journal of Climate*, 27, 2983-2999.
- 300 Trapp, R. J., Diffsenbaugh, N. S., & Gluhovsky, A. (2009, Jan). Transient response
301 of severe thunderstorm forcing to elevated greenhouse gas concentrations.
302 *Geophysical Research Letters*, 36(1). Retrieved from [http://dx.doi.org/
303 10.1029/2008GL036203](http://dx.doi.org/10.1029/2008GL036203) doi: 10.1029/2008gl036203